TDS study of deuterium distribution in 3^{rd} generation high strength steels as a function of charging conditions and cold rolling

A. Pushparasah, F. Martin, Q. Auzoux, T. Dieudonne, S. Cobo, L. Moli-Sanchez, K. Wolski

TDS study of deuterium distribution in 3rd generation high strength steels as a function of charging conditions and cold rolling

A. Pushparasah[1,4], F. Martin[1], Q. Auzoux[1], T. Dieudonné[2], S. Cobo[2], L. Moli-Sanchez[3], K. Wolski[4]

[1]*DEN-Service de la Corrosion et du Comportement des Matériaux dans leur Environnement (SCCME), CEA, Université Paris-Saclay, F-91191, Gif-sur-Yvette, France*

[2] *ArcelorMittal Global Research and Development Maizières Automotive Product, Voie Romaine, F-57280 Maizières-lès-Metz, France*

[3]*ArcelorMittal Global Research and Development Gent, Technologiepark 935, B-9052 Zwijnaarde, Belgium*

[4]*Ecole des Mines de Saint-Etienne, 158 Cours Fauriel, Centre SMS, LGF UMR CNRS 5307, F-42023 Saint-Etienne, France*

Abstract

Two 3rd generation steels were studied: an austenitic-ferritic MnAl steel and an austenitic-martensitic quenched and partitioned (Q&P) steel. Hydrogen absorption during elaboration was simulated by exposing the steels to deuterium atmosphere during their final thermal treatment. Nitrogen-exposed specimens were also deuterium cathodically charged in order to simulate hydrogen entry in the steels during an optional electrogalvanization process. Thermal desorption mass spectrometry (TDS), combined with aging at room temperature and cold rolling, was used to study diffusion and trapping. The evolution of different TDS spectral contributions with aging and cold rolling allowed educated guesses on their origin. Peaks specific to martensitic transformation were identified.

Keywords: hydrogen, deuterium, high strength steels, cold rolling, thermal desorption spectrometry

Introduction

Third generation high strength steels have been designed to answer ever more competitive assessments for structural parts in the automotive industry. The TRansformation Induced Plasticity (TRIP) steels combine high mechanical properties with good formability and ductility due to the high amount of residual austenite which transforms (partly or fully) into martensite with strain (stamping or shock). During the industrial elaboration process of such steels, two entry routes for hydrogen were identified: (i) the final thermal treatment, performed in a reducing atmosphere at high temperatures [Escobar2012], and (ii) in some cases, electrogalvanization at low temperatures [Georges2009, DelPupo2015, Townsend1981]. Sensitivity of TRIP-aided steels to hydrogen embrittlement (HE) was demonstrated on elder generations of steels. Different mechanisms accounting for hydrogen embrittlement of such steels have been proposed in literature, but most agree on the fact that fresh strain-induced martensite may

be responsible for HE cracks initiation [Ronevich2010, Lovicu2012, Ronevich2012, Laureys2016, Silverstein2017, Li2017, Zhu2013]. The embrittlement mechanism relies on the difference in both diffusivity and, even more, solubility of hydrogen in the austenite and martensite phases, potentially giving rise to local hydrogen overconcentrations in the freshly formed martensite [Silverstein2017a]. However, the re-distribution of hydrogen during the phase transformation occurring while straining the TRIP steels is far from being understood [Escobar2012]: hydrogen may either effuse via the fresh martensite [Prioul1984, Ryu2012, Kim2012], or be trapped at new dislocations emitted in the martensite or ferrite [Escobar2012, Kim2012] or at new types of traps like new interfaces [Escobar2012, Li2017, Silverstein2017a], or stay in the remaining austenitic phase [Sojka2011, Sugimoto2009].

Before considering investigations on the re-distribution of hydrogen during straining in such complex materials, studying the initial distribution of hydrogen in terms of trapping and lattice hydrogen is the first step towards understanding. It has been demonstrated (by electrochemical permeation [Turnbull1994, Owczarek2000, Zackrozimsky2002], *in situ* permeation in SIMS [Sobol2016] or SKPFM [Nagashima2017]) that diffusion in the ferritic or martensitic matrix of dual phase steels is very quick. This leads to rapid saturation of the matrix with hydrogen and provides a hydrogen flux to traps or austenite grains. Low energy traps, that could be dislocations [Ryu2012, Escobar2012, Ronevich2012], have been evidenced by TDS studies on TRIP steels. Such traps do not prevent hydrogen desorption from the material at room temperature [Ronevich2012, Ryu2012]. Martensite/martensite grain boundaries could trap hydrogen, as shown by the silver decoration method [Nagashima2017]. Nonetheless the presence of austenitic grains seems to be the main source of trapping in such dual phase steels [Owczarek2000, Zackroczymski2002, Turnbull1994, Olden2008, Sugimoto2009, Gu2002, Ryu2012, Escobar2012]. The austenite grains themselves [Turbull1994, Sugimoto2009, Gu2002, Zackrozimsky2002] and/or their interface with the matrix [Turnbull1994] can trap hydrogen, provided it is not destabilized by the presence of hydrogen [Teus2008, Silverstein2017b].

The first part of our work was dedicated to further identify the potential different trap sites in two different third generation TRIP-aided steels, function of the hydrogen entry route, since temperature and hydrogen surface fugacity may play a role on trapping or traps density modifications [Sobol2017, Liang2018, Silverstein2015]. TDS analysis involving deuterium exposures coupled with room temperature aging was the method chosen for this study. The second part of the paper focuses on the effect of strain, and more specifically phase transformation effects on the TDS thermograms.

Materials and methods

The base materials used in this study are: (i) a ferritic-austenitic MnAl steel and (ii) a martensitic-austenitic steel “Quenched and Partitioned” (thereafter referred to as Q&P). Their chemical compositions are given in Table 1, expressed in weight % (wt.%).

	C	Mn	Al	Si	Nb	S	P
MnAl	0.12	5	1.8	0.5	0.03	<0.003	0.012
Q&P	0.3	2.5	-	2.4	-	<0.003	0.012

Table 1: composition (wt.%) of the two studied high strength steels, Fe balance.

These 3rd generation high strength steels were hot rolled, cold rolled down to 1 mm thick sheets then submitted to a final heat treatment in order to obtain the desired microstructure. The thermal treatment conditions are detailed in Figure 1. For the MnAl it consisted basically in an isotherm at 740°C (above the austenite transus A_{c1}), aiming at nucleating and growing austenite grains in the ferritic matrix, followed by quenching. The composition of the alloy was chosen so that the austenite is metastable at room temperature and can transform into martensite when deformed. The Q&P thermal treatment consisted in full austenitization (temperature above A_{c3}), followed by a controlled quenching in the [Mf; Ms] temperature range in order to form some martensite, followed by a partitioning during which the remaining austenite is stabilized. The treatment is ended with a full quench of the sheet.

Scanning electron microscopy (SEM) observations of the obtained microstructures, after nital etching (see Figure 2) show that MnAl alloy exhibits small austenite grains (0.5 to 1 µm in diameter) embedded in the ferrite matrix, separated by about 1 µm from each other. X-ray diffraction (XRD) measurements combined with Rietveld refinement indicate an austenite fraction of 26 wt.% after the final thermal treatment (see Table 2). The Q&P steel presents a complex martensitic microstructure. XRD analysis indicates about 18 wt.% of residual austenite in the Q&P steel (see Table 2). EBSD phase identification was only able to count 2-to-5% of austenite, mainly in the blocky form, suggesting the rest of the austenite is too small to be identified by this technique, in the form of needles or films between martensite laths.

Two different ways of introducing deuterium (^{2}H or D) in these steels were chosen. Deuterium was used to minimize artifacts due to hydrogen surface pollution, specimen preparation or elaboration hydrogen prior to heat treatment in order to focus on the distribution of hydrogen species (deuterium here) according to their origin. First, the specimens thereafter referred to as High Temperature (HT) were exposed, during the whole duration of the final heat treatment (see Figure 1), to pure D_2 gas at atmospheric pressure. Deuterium incorporation during the thermal treatment did not affect the austenite fraction (see Table 2). HT-specimens were polished down to mirror finish before being analyzed. Second, another set of specimens, thereafter referred to as Low Temperature (LT) were exposed to pure N_2 gas atmosphere during the final heat treatment as previously (see Figure 1), then polished and cathodically charged with deuterium in 0.1 M NaOD solution under a current density of -10 mA/cm² for 1 hour at 80 °C. To prevent deuterium desorption before the analysis, all specimens were held in liquid nitrogen until characterized. XRD indicated that the austenite fraction was unaffected by this procedure.

Part of the sheets were cut and cold rolled in the long transverse direction up to 30% equivalent strain (26% thickness reduction) at room temperature. The austenite fraction was measured by XRD before, and after cold rolling, as reported in Table 2..

A home-designed and -made thermal desorption mass spectrometer (TDS) was used in this study [Hurley2015, Hurley2016]. 10x10 mm² specimens machined by spark erosion were used. The temperature was measured by a type-K thermocouple located as close as possible to the specimen located inside a quartz tube under secondary vacuum. Specimens were heated up to 1000 °C at a rate of 10 °C.min^{-1}. Specimen temperature evolution with time was monitored as well as ionic current of the mass spectrometer, for m/z ratio of 4.

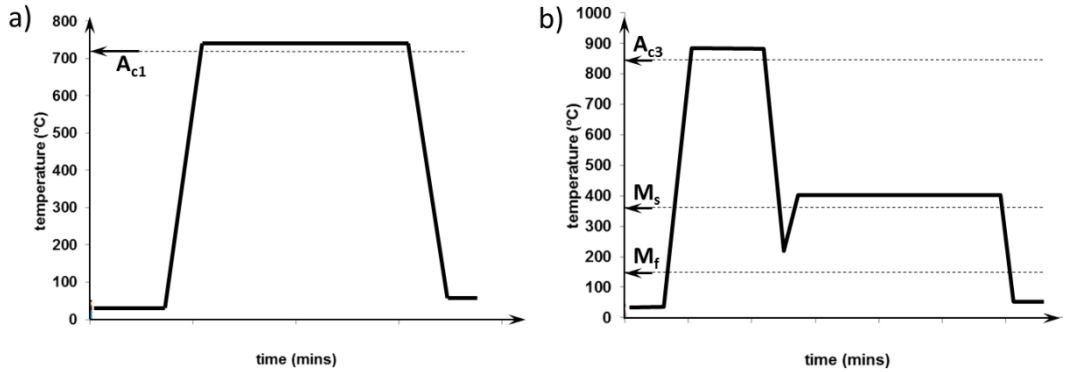

Figure 1: typical final thermal treatments applied to a) MnAl steel and b) Q&P steel.

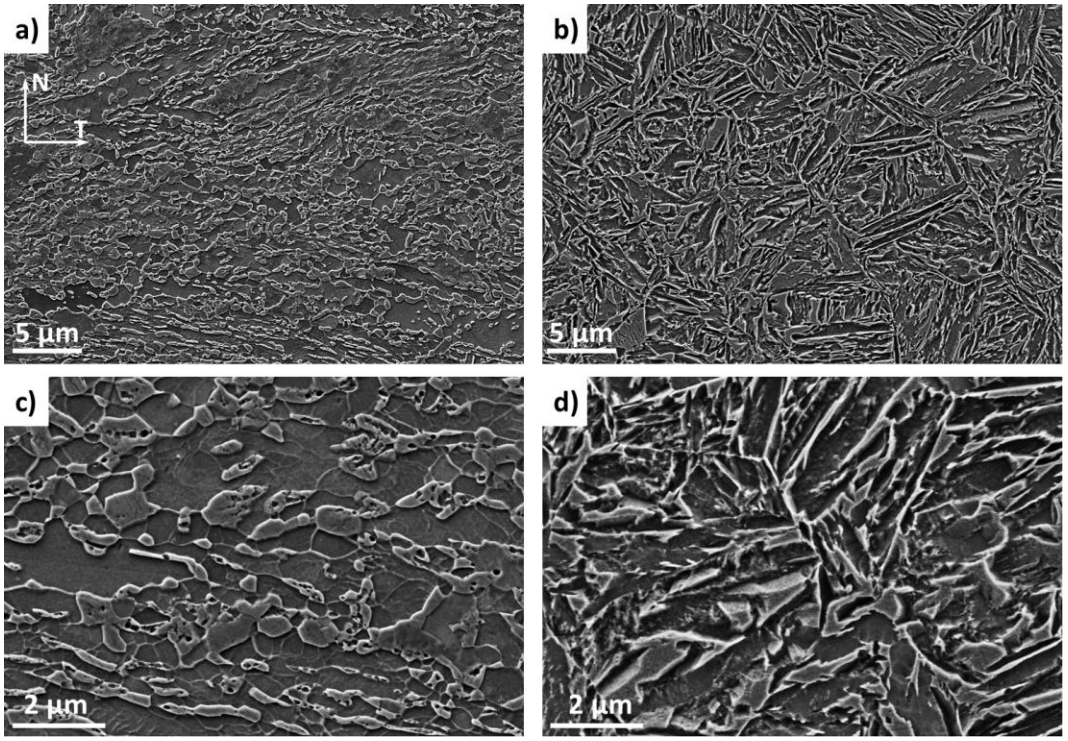

Figure 2: SEM (secondary electrons) micrographs after nital etching of a),c) MnAl steel and b),d) Q&P steel at same magnifications (a-b and c-d). All micrographs are oriented as indicated in a). For MnAl, austenite grains appear in relief due to relatively slower etching than ferrite grains.

Fraction of austenite (wt.%)	before cold rolling	after cold rolling
MnAl treated in N_2 atmosphere	26	5
MnAl treated in D_2 atmosphere	27	3
Q&P treated in N_2 atmosphere	18	9
Q&P treated in D_2 atmosphere	18	7

Table 2: fraction of austenite (in wt. %) in the two steels after the thermal treatment in N_2 or D_2 atmosphere, before and after 30% equivalent strain cold rolling. Values are issued from XRD measures and Rietveld refinement.

Results

Initial deuterium distributions and desorption during aging at room temperature

The deuterium desorption flux from MnAl and Q&P HT-specimens during TDS temperature ramp are gathered in Figure 3, showing different peaks in the thermograms. Different contributions are clearly visible on thermograms recorded on room temperature-aged specimens (see Figure 3, color curves). The spectra for both materials have similarities and present two contributions in the 170-280 °C range.
For the MnAl steel (see Figure 3.a), only two peaks are observed, centered at 210 °C and 250-280 °C. The peak at 210 °C decreases with aging time and disappears after 2 weeks, whereas the second contribution around 250-280 °C also decreases in intensity but is still detected after two weeks aging. The associated deuterium fully desorbs from the specimen within the next eight weeks.
For the Q&P steel (see Figure 3.b), the two main peaks are centered at 170 °C and 210 °C (see spectrum after 24 h aging at room temperature). The first one decreases rapidly with aging time, disappearing within one week. The second one decreases also, but to a lower extent and remains after four weeks aging – but disappears within the next six weeks of aging. A shift of this peak towards higher temperatures is observed with aging time – from 210 °C to 250 °C. Contrary to the MnAl steel, the spectra obtained on the Q&P alloy present an additional peak at much higher temperature centered at 500-520 °C. This peak seems stable: after 1 week, and even after 4 or 10 weeks at room temperature the peak intensity and position remain almost unaffected (see insert in Figure 3.b).

TDS spectra recorded on LT-specimens after cathodic charging at 80°C are gathered in Figure 4. As for HT-specimens, the consequences of room temperature aging on the residual hydrogen content were studied. A straightforward comparison with spectra obtained on HT-specimens gives rise to following considerations: (i) before aging, both high and low temperature-charged specimen thermograms exhibit similar peak positions, (ii) for the Q&P LT-specimens no peak is observed above 400 °C contrary to Q&P HT-specimens, (iii) after 48 hours of aging at 20 °C, the LT-specimens do not contain deuterium anymore and consequently (iv) room temperature desorption rate is higher for LT-specimens. In addition, quantitative analysis of the different spectra obtained for low temperature charging indicates that the low temperature charging procedure induced a higher deuterium uptake as compared to high temperature exposure for the MnAl steel

(0.21 vs 0.06 wt.ppm), whereas the contrary was observed for the Q&P steel (0.05 vs 0.21 wt.ppm).

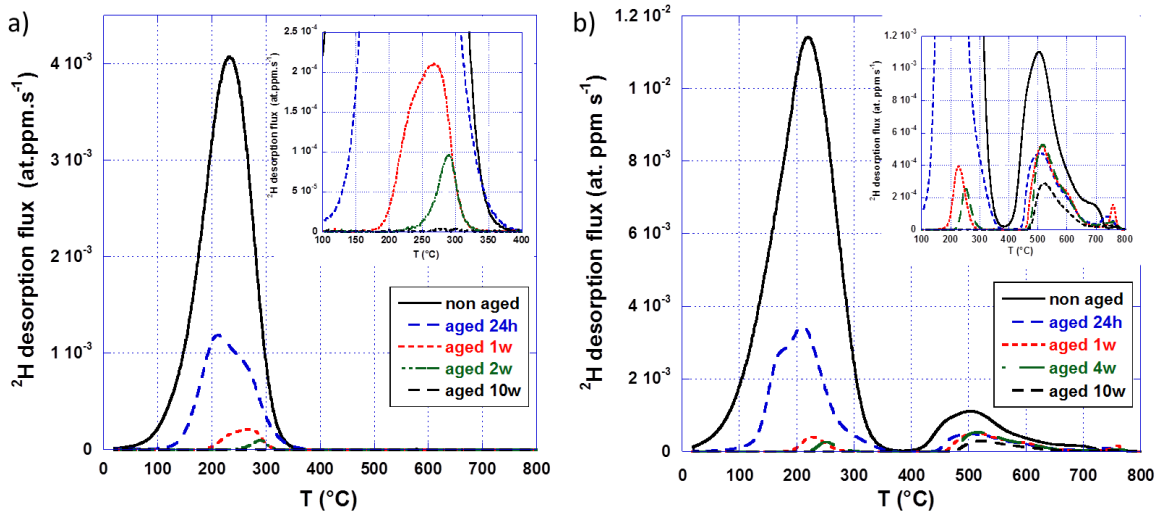

Figure 3: TDS deuterium desorption thermograms performed at 10 °C.min^{-1} on a) MnAl and b) Q&P steels exposed to D_2 atmosphere during their final thermal treatment (black line, just after treatment). Specimens were aged at room temperature for 24 hours, 1 week, 2 or 4 weeks, and 10 weeks and corresponding thermograms are drawn in blue, red, green and black dashed lines respectively.

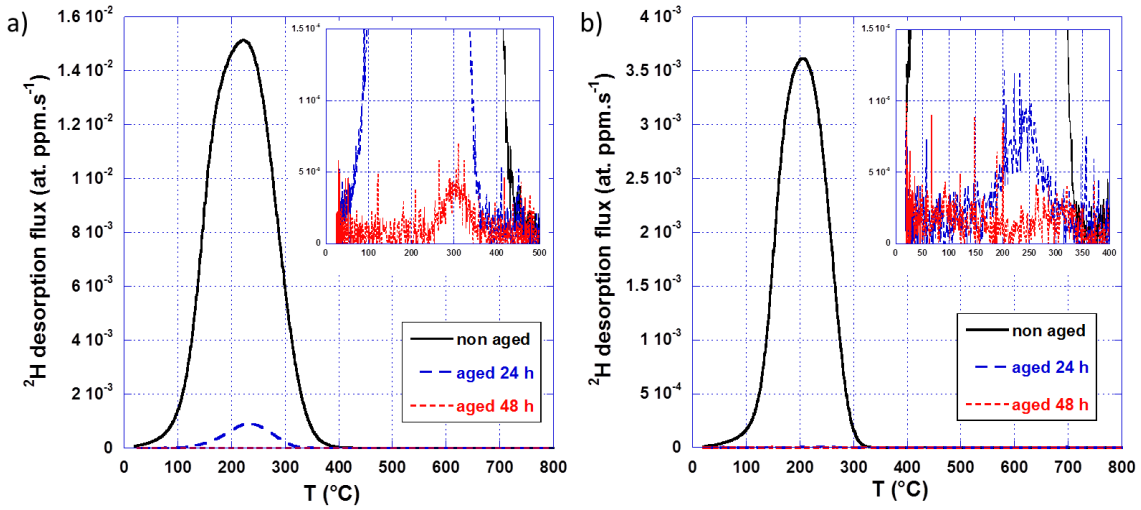

Figure 4: TDS deuterium desorption thermograms recorded on a) MnAl and b) Q&P steels treated under N_2 atmosphere then cathodically charged for 1 hour at 80 °C in 0.1M NaOD solution. The thermograms obtained just after deuterium charging are in black; those obtained after 24 h and 48 h duration room temperature aging are in blue and red, respectively.

Effect of cold rolling on the deuterium desorption

The thermograms obtained on MnAl HT-specimens are presented in Figure 5.a. Cold rolling induced a shift of the main peak towards higher temperatures, its sharpening and increase in intensity. The higher amount of deuterium desorbing during TDS from the cold rolled specimen as compared with the initial specimen was probably due to slight differences in deuterium distribution in the initial sheet, or a reduced loss of deuterium during the initial TDS pumping before actual analysis starts (trapping effect). After cold rolling, the low temperature foot of the desorption peak disappeared, showing negligible desorption at temperatures below 150 °C under the experimental TDS conditions, whereas significant desorption was observed at 100 °C before cold rolling. This peak, centered at 230 °C for non-aged specimens, shifted progressively with aging time towards higher temperatures (e.g. 260 °C after four weeks aging). It suggests that the initial peak (black continuous line in Figure 5.a) may be the convolution of two peaks: one centered at 230 °C, the other being centered 260 °C.
Figure 5.b gathers the thermograms obtained on the Q&P HT-specimens before and after cold rolling, followed by aging at room temperature. As for the MnAl, cold rolling induced a shift of the peak towards higher temperatures, as well as its sharpening and increase in intensity. The amount of deuterium desorbing corresponding to this peak decreased slowly with aging duration, suggesting a room temperature desorption from the sites associated with this peak. Note that the peak around 500 °C is quite erratic in its position and intensity, but globally does not change much with cold rolling or aging duration.

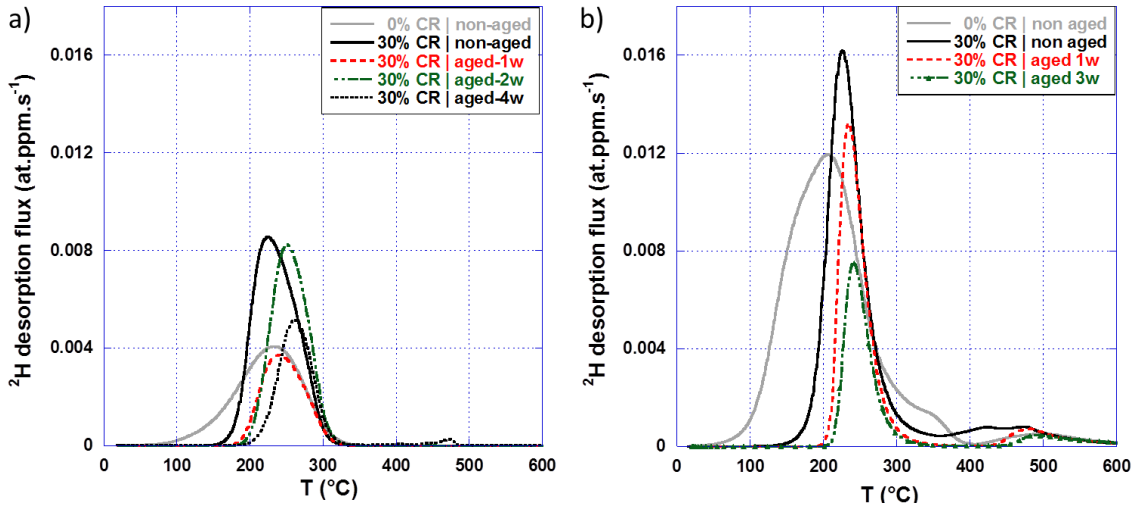

Figure 5: TDS deuterium desorption thermograms obtained on a) MnAl and b) Q&P steels exposed to D_2 atmosphere during the thermal treatment (HT-specimens), before (light grey) and after (black) cold rolling (CR) up to 30 % equivalent strain, then aged (color) at room temperature during different periods of time.

Discussion

General comments on the collected TDS spectra

Based on literature data on the lattice/interstitial diffusion coefficient of hydrogen in the ferritic or martensitic phases at room temperature [Turnbull1994, Zakroczymski2002], the TDS spectral contribution of lattice/interstitial hydrogen in ferrite or martensite should be negligible. Numerical simulations – not presented here – showed indeed that most of the lattice hydrogen effuses out of the specimen during the transfer from liquid nitrogen holder to TDS experiment, and that remaining desorbing hydrogen would form a peak at room temperature only. The experimental spectra obtained on both materials do not show any desorption peak at room temperature, but a very low desorption flux that could indeed be the signature of ferrite or martensite interstitial deuterium still desorbing or weakly-trapped hydrogen desorption contribution. It comes that the peaks observed on the thermograms above 100 °C do not correspond to interstitial deuterium in ferritic or martensitic phases.

Some cathodic charging conditions, enhanced by recombination poisons for instance, induce so high surface hydrogen fugacities that significant amounts (or fluxes) of hydrogen enter the steels. Such charging can result in phase changes [Sobol2017, Silverstein2015] or dislocations emission [Liang2018]. In order to prevent these artifacts, the charging conditions used in our study were relatively smooth (a current density of 10 $mA.cm^{-2}$ in pure 0.1M NaOD aqueous solution).

Deuterium distribution differences induced by the charging mode

TDS spectra recorded on both MnAl and Q&P HT- and LT-specimens present a broad peak around 200 °C, which seems to result from two contributions. The decrease of the intensity of these contributions with aging duration at room temperature indicates reversible trapping. The peak position shift towards higher temperatures after aging at room temperature suggests different detrapping activation energies for the two contributions: the higher the contribution temperature, the lower the desorption rate and the higher the detrapping (or binding) energy. For both MnAl and Q&P steels, broad peaks located at around 200 °C obtained on HT- and LT-specimens before aging are similar in shape, which means that desorption kinetics from LT- and HT-specimens are similar around 200°C. However, desorption kinetics at room temperature is much quicker from LT-specimens than from HT-specimens. It indicates that deuterium detrapping activation energy was lower in LT-specimens than in HT-specimens. Consequently, one can infer that deuterium distribution in the trapping sites resulting from charging at high or low temperature differ from one to another. Clearly, the deuterium absorption during HT thermal treatment resulted in a stronger trapping than the LT cathodic charging at 80°C.

The TDS peak observed at around 450 °C on the Q&P steel exposed to deuterium at high temperature was not observed after cathodic charging at 80 °C. Two hypotheses could

account for this difference: (i) the associated trap sites are not filled at 80 °C because of a too high trapping activation energy or (ii) the associated traps do not exist in the N_2-exposed specimen because they arise specifically from the martensitic transformation occurring in a deuterium (or hydrogen) charged steel. The final thermal treatment consists in a full austenitization stage (with deuterium uptake in the austenitic phase) followed by a partial quenching, inducing the formation of martensite. During the martensitic transformation, some of the deuterium formerly in the austenite is now in the martensite and can diffuse out of it or be trapped at newly generated defects. These defects could be austenite-martensite interfaces, which are also generated in N_2-exposed specimen, or could be specific crystallographic defects like vacancies, vacancies clusters or nanocavities resulting from the phase transformation of the deuterium charged austenite. Literature data referring to hydrogen trapping at such defects report high binding energies that may be compatible with current observations [Hayward2012]. Such defects have nonetheless not been evidenced in the present steels. Further investigations are therefore needed to discriminate between the two hypotheses. These two hypotheses are also consistent with the fact that no peak was recorded for MnAl HT- and LT-specimens above 400 °C till 1000 °C. But this result questions the assignment of the peak around 450°C to trapping in austenite suggested by Escobar *et al.* in testing conditions relatively close to ours [Escobar2012]. As the MnAl steel presently studied contained 26 wt.% austenite, it appears that, in our experimental conditions, deuterium detrapping from austenite certainly occurs in the [180-300 °C] range.

Deuterium redistribution due to cold rolling of HT-specimens

Cold rolling of both MnAl and Q&P HT specimens induced a shift and a sharpening of the broad TDS desorption peak at around 200 °C towards higher temperature. This shift is not attributable to the specimen thickness reduction due to cold rolling because it would then be inversely shifted towards lower temperature. These observations are consistent with deuterium formerly weakly trapped (peak contribution around 180 °C) being captured by some new traps created during cold rolling. These sites could be new dislocations or new austenite-martensite interfaces arising from the austenite strain-induced transformation. Such a mechanism is also consistent with the fact that the overall deuterium concentration in the material was not affected by cold rolling (within the data scatter). At least, desorption of hydrogen was not significant during this step, discarding the high effusion theory from the material due to the martensitic transformation [Ryu2012]. The peak contribution found prior to cold rolling at around 180 °C would thus be assigned to trapping in austenite grains or at austenite-ferrite (or austenite-martensite) interfaces. This peak position for austenite is consistent with the fact that the austenite grains embedded in the ferritic or martensitic matrix are very small, which accelerates desorption most significantly in comparison to pure austenitic materials.

The possibility of trapping at vacancies that would have been formed by the martensitic transformation of deuterium charged austenite during cold rolling cannot be discarded either. However, based on previous discussion on Q&P steel, they would not be associated with a peak around 250 °C but rather at higher temperature. The peak at 250 °C could therefore be associated with dislocations or austenite-martensite interfaces.

Dislocations are present in the material before cold rolling and a peak contribution was also found around 250 °C prior to deformation. Nevertheless, the desorption kinetics at room temperature after cold rolling is lower than before cold rolling. It may be due to the drastic increase in trap density induced by cold rolling causing a detrapping-retrapping process, thus slowing down desorption.

The TDS peak observed at around 450 °C on the Q&P HT-specimens was not affected by the cold rolling and did not decrease during the three-weeks aging at room temperature (differences stay within the reproducibility range of the experiment). After cold rolling, only 7 wt.% austenite remains as compared to the initial 18 wt.%. Consequently, the peak around 450 °C could not reasonably be assigned to deuterium trapped in the austenite phase. The deuterium located at the corresponding sites is in a very stable location, i.e. irreversible trap sites. As mentioned earlier, this observation is compatible with trapping at vacancies, vacancies clusters, nanovoids or nanocavities.

Conclusions

Reversible trapping of hydrogen in a Mn-Al austenite-ferrite steel and a Q&P austenite-martensite steel was evidenced after both cathodic charging at 80 °C and gaseous charging during the thermal treatment. Results obtained on specimens aged at room temperature and cold rolled specimens suggested that the corresponding trapping sites are most probably austenite-ferrite (or austenite-martensite) interfaces and dislocations. Contrary to previous literature reports, the detrapping from residual austenite was assigned to relatively low temperature peak contribution. Room temperature desorption kinetics was much slower after high temperature than low temperature charging, indicating a stronger trapping at higher temperature. Cold rolling also reduced the desorption kinetics, which may be caused by the drastic trap density increase due to new dislocations and interfaces.

For the Q&P steel charged at high temperature, an additional irreversible contribution to trapping was evidenced, probably created by the synergy between the presence of hydrogen in austenite at high temperature and the quenching. Speculations are made on the nature of such traps, which could be nanovoids, nanocavities or multiple H-vacancies clusters.

Acknowledgements

The authors would like to kindly acknowledge M. Hell from ArcelorMittal Global R&D, Maizières-lès-Metz, France, for the XRD analyses and data treatment.

References

[Delpupo2015] M. N. Delpupo, M. N. Inés, G. Candia, C. Asmus, and G. A. Mansilla, Procedia Mater. Sci. 9 (2015) pp.171-176, Proceedings of the International Congress of Science and Technology of Metallurgy and Materials, SAM – CONAMET 2014.

[Escobar2012] D. Pérez Escobar, T. Depover, L. Duprez, K. Verbeken and M. Verhaege, Acta Mater. 60 (2012) pp. 2593-2605.

[Georges2009] C. Georges and T. Sturel, in : Effect of Hydrogen on materials – Proceedings of the International Hydrogen Conference, Grand Teton Natl. Park, Wy, Sept. 07-10 2008, Edts. B. Somerday, P. Sofronis and R. Jones.

[Gu2002] J.L. Gu, K.D. Chang, H.S. Fang and B.Z. Bai, ISIJ Intern. 42 (2002) pp. 1560-1564

[Hayward2012] E. Hayward , B. Beeler and C. Deo, Philosophical Magazine Letters 92 (2012) pp. 217-225.

[Hurley2015] C. Hurley, F. Martin, L. Marchetti, J. Chêne, C. Blanc and E. Andrieu, Int. J. Hydrogen Energy 40 (2015) pp. 3402-3414.

[Hurley2016] C. Hurley, F. Martin, L. Marchetti, J. Chêne, C. Blanc and E. Andrieu, Int. J. Hydrogen Energy 41 (2016) pp. 17145-17153.

[Kim2012] S.J. Kim, D.W. Yun, D.W. Choo and K.Y. Kim, Electrochem. Comm. 24 (2012) pp. 112-115.

[Laureys2016] A. Laureys, T. Depover, R. Petrov and K. Verbeken, Mater. Charact. 112 (2016) pp. 169-179.

[Li2017] Y. Li, W. Li, J.C. Hu, H.M. Song and X.J. JinInt. J. Plasticity 88 (2017) pp. 53-59.

[Liang2018] X.Z. Liang, M.F. Dodge, S. Kabra, J.F. Kelleher, T.L. Lee and H.B. Dong, Scripta Mater. 143 (2018) pp. 20-24.

[Lovicu2012] G. Lovicu, M. Bottazzi, F. D'Aiuto, M. De Sanctis, A. Dimatteo, C. Santus and R. Valentini, Metall. Mater. Trans. A 43A (2012) pp. 4074-4087.

[Nagashima2017] T. Nagashima, M. Koyama, A. Bashir, M. Rohwerder, C.C. Tasan, E. Akiyama, D. Raabe and K. Tsuzaki, Mater. Corros. 68 (2017) pp. 306-310.

[Olden2008] V. Olden, C. Thaulow and R. Johnsen, Mater. Design 29 (2008) pp. 1934-1948.

[Owczarek2000] E. Owczarek and T. Zakroczymski, Acta. Mater. 48 (2000) pp. 3059-3070.

[Prioul1984] C. Prioul, C.A.V. de A. Rodrigues, M. Groos and P. Azou, Scripta Metall. 18 (1984) pp. 601-604.

[Ronevich2010] J. Ronevich, J. Speer and D. Matlock, SAE Int. J. Mater. Manuf. 3 (2010) pp. 255-267.

[Ronevich2012] J.A. Ronevich, B.C. De Cooman, J.G. Speer, E. De Moor and D.K. Matlock, Metall. Mater. Trans. A 43A (2012) pp.2293-2301.

[Ryu2012] J.H. Ryu, Y.S. Chun, C.S. Lee, H.K.D.H. Bhadeshia and D.W. Suh, Acta Mater. 60 (2012) pp.4085-4092.

[Silverstein2015] R. Silverstein, D. Eliezer, B. Glam, S. Eliezer and D. Moreno, J. Alloys Compds. 648 (2015) pp. 601-608.

[Silverstein2017a] R. Silverstein and D. Eliezer, J. Alloys Compds. 720 (2017) pp. 451-459.

[Silverstein2017b] R. Silverstein and D. Eliezer, Mater. Sci. Eng. A 684 (2017) pp. 64-70.

[Sobol2016] O. Sobol, F. Straub, Th. Wirth, G. Holzlechner, Th. Boellinghaus and W.E.S. Unger, Sci. Rep. 6, 19929.

[Sobol2017] O. Sobol,G. Nolze, R. Saliwan-Neumann, D. Eliezer, Th. Boellinghaus and W.E.S. Unger, Int. J. Hydrogen Energy 42 (2017) pp. 25114-25120.

[Sojka2011] J. Sojka, V. Vodarek, I. Schindler, C. Ly, M. Jerome, P. Vanova, N. Rucassier and A. Wenglorzova, Corros. Sci. 53 (2011) pp. 2575-2581.

[Sugimoto2009] K.I. Sugimoto, Mater. Sci. Technol. 25 (2009) pp. 1108-1117.

[Teus2008] S.M. Teus, V.N. Shyvanyuk and V.G. Gavriljuk, Mater. Sci. Eng. A 497 (2008) 290–294

[Townsend1981] H.E. Townsend, Corrosion-NACE 37 (1981) pp. 115-120.

[Turnbull1994] A. Turnbull and R.B. Hutchings, Mater. Sci. Eng. A 177 (1994) pp. 161-171.

[Zakroczymski2002] T. Zakroczymski and E. Owczarek, Acta Mater. 50 (2002) pp. 2701–2713.

[Zhu2013] X. Zhu, W. Li, H. Zhao and X. Jin, Int. J. Hydrogen Energy 38 (2013) pp. 10694-10703.

[Zhu2016] X. Zhu, K. Zhang, W. Li and X. Jin, Mater. Sci. Eng. A 658 (2016) pp. 400-408.